Dynamic Light Scattering Study on Reentrant Sol−Gel Transition of Poly(vinyl alcohol)−Congo Red Complex in Aqueous Media

Masayuki Tsujimoto

Department of Polymer Science and Engineering, Kyoto Institute of Technology, Matsugasaki, Sakyo-ku, Kyoto 606-8585, Japan

Mitsuhiro Shibayama*

Neutron Scattering Laboratory, Institute for Solid State Physics, The University of Tokyo, Tokai, Naka-gun, Ibaraki 319-1106, Japan

Received July 6, 2001; Revised Manuscript Received November 20, 2001

ABSTRACT: The poly(vinyl alcohol)−Congo Red (PVA/CR) complex in aqueous solutions exhibited a reentrant sol−gel transition at ambient temperature by increasing the CR concentration, C_{CR}, when the PVA concentration was near the chain overlap concentration ($C_{PVA} \approx 455$ mM). The system was in the sol state at $C_{CR} \leq 1.0$ mM and $10.0 \leq C_{CR} \leq 30.0$ mM, while it underwent gelation at two C_{CR} regions: $1.5 \leq C_{CR} \leq 9.0$ mM and 35 mM $\leq C_{CR}$. This reentrant transition has been investigated microscopically by means of dynamic light scattering. Speckle patterns appeared exclusively in the gel phase. The reentrant sol−gel transition was also demonstrated by a shape change of the time−intensity correlation function (ICF), which varied from a stretched-exponential function for sol states to a power-law function for gel states. The variations of the correlation length ξ and the power-law exponent, n, in ICF have been extensively discussed.

Introduction

Poly(vinyl alcohol) (PVA) is known as a polymer capable of complexation with borate ions,[1] cupric ions,[2] and some other inorganic ions, such as titanate,[3] antimonate,[4] and vanadate ions.[5−8] The properties of these polymer−ion complex aqueous solutions are similar to those of polyelectrolytes when the attached charges are stable. However, since these attached charges are usually in a complexation equilibrium, the charged groups can be easily dissociated from the polymer chain by changing their ionic environment. This results in a drastic change in the rheological properties of the polymer solution. If the attached charge is coupled with another polymer segment (i.e., dicomplexation), a cross-link is formed, which leads to a clustering, phase demixing, and/or gelation.[8−10]

Congo Red (CR) shown in Figure 1a is also a cross-linking reagent of PVA. CR is ionized in aqueous solutions.[11] The complexation process can be classified into two steps, one being monocomplexation and the other dicomplexation.[12−14] The monocomplexation, an attaching of a CR ion to a unit of a PVA chain, leads to a polyelectrolyte-type behavior of the polymer chain (Figure 1b). When another monomer unit of a polymer chain is complexed to the attached CR ion, a dicomplexation occurs, and the complexed ion behaves as a cross-link (Figure 1c). However, these complexations are usually on a delicate balance of complexation equilibrium as discussed by Leibler et al.[9] for PVA borate ion complexes. Therefore, it is needless to mention that the complexation equilibrium depends on PVA concentration, C_{PVA}, CR concentration, C_{CR}, and temperature, T. Figure 2 shows the sol−gel phase diagram for PVA/CR aqueous solutions at 20 °C.[12] The sol region becomes large by increasing T, and no gel phase is observed for

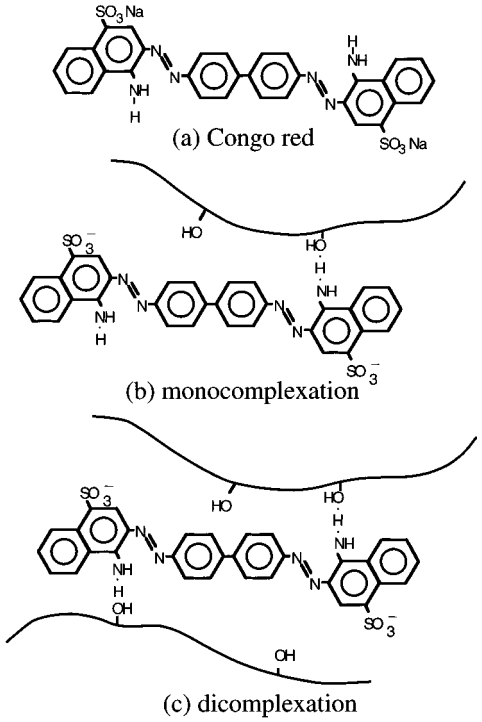

Figure 1. Chemical structures of (a) Congo Red, (b) PVA/CR monocomplex, and (c) dicomplex.

$T > 45$ °C. Hence, this system undergoes a sol−gel transition by changing either temperature or concentration of the solutes. One of the characteristic features of this phase diagram, however, lies in *a reentrant type sol−gel transition*. In the region $C_{CR} \leq 10$ mM, the sol−gel transition border shifts to the lower concentration of C_{PVA}. This means that the PVA chains are expanded by ionization which is brought by CR. On the other hand, in the region $10 \leq C_{CR} \leq 30$ mM, intrachain cross-linking becomes dominant, resulting in shrinking of

* To whom correspondence should be addressed.

10.1021/ma011175b CCC: $22.00
Published on Web 01/18/2002

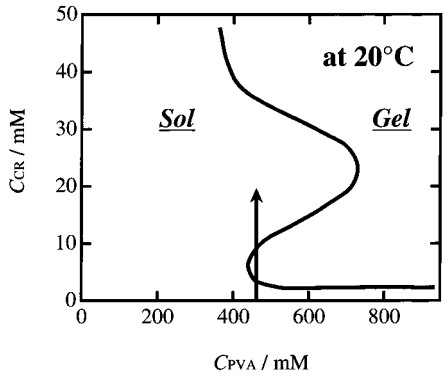

Figure 2. Phase diagram of the reentrant sol−gel transition for PVA/CR complexes in aqueous solutions obtained at 20 °C.

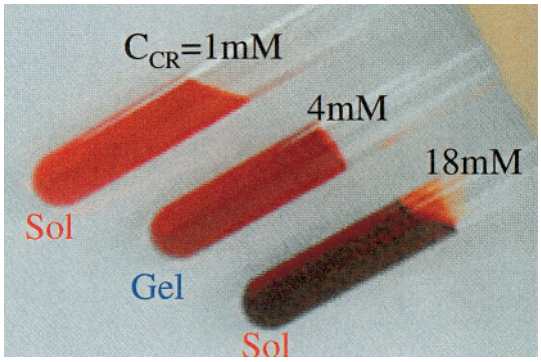

Figure 3. Photograph showing sol and gel states of PVA/CR complexes.

PVA chains. The following region, i.e., 30 mM ≤ C_{CR}, is characterized by the region where electrostatic screening is dominant. The reentrant sol−gel transition is more clearly demonstrated in Figure 3. It shows a photograph of PVA/CR aqueous solutions with C_{PVA} = 455 mM and C_{CR} = 1.0, 4.0, and 18 mM in test tubes at 20 °C. When tilting the test tubes, the meniscus of the PVA/CR complexes with C_{CR} = 4.0 mM did not move. On the other hand, the meniscus of the others changed so as to keep it to be horizontal. This is a clear indication of whether the system is in the sol or gel state. It should be noted that this macroscopic sol−gel transition is reproducible with respect to C_{CR}.

In a previous paper,[15] we investigated temperature-induced and concentration-induced sol−gel transitions of PVA−CR aqueous complexes by dynamic light scattering (DLS). It was demonstrated that thermo- and lioreversible sol−gel transition threshold can be determined by DLS, similar to the case of chemical gels, such as poly(*N*-isopropylacrylamide) gels[16,17] and silica gels.[18] In both cases, gelation was accompanied by an appearance of a speckle pattern in laser scattering and a power-law behavior in the intensity−time correlation function. It was also disclosed that the temperature-induced sol−gel transition accompanies a gradual change of correlation length, ξ, while the concentration-induced sol−gel transition exhibits a divergence of ξ at the transition threshold. The objective of this paper is to examine whether such characteristic features of gelation are observed in a system undergoing a reentrant sol−gel transition and to elucidate the physical meaning of the reentrant sol−gel transition.

Experimental Section

Samples. A series of poly(vinyl alcohol)−Congo Red (PVA/CR) aqueous solutions were prepared. PVA powder (the degree of polymerization = 1800 and the degree of saponification = 99.96 mol %), kindly supplied by Nippon Gosei Co. Ltd., Osaka, Japan, was used without further purification. CR was purchased from Wako Chemical Co. Ltd., Tokyo. CR is a synthetic dye and is known as a thermoreversible cross-linker of PVA in aqueous solutions. 1.36 M PVA and 40 mM CR aqueous solutions were separately prepared by dissolving them in boiling distilled water and filtering through a 0.45 μm filter. Prescribed amounts of two solutions were mixed together at ca. 80 °C, and a homogeneous solution of PVA/CR with various ratios, C_{PVA}/C_{CR}, was obtained, where C_{PVA} and C_{CR} are concentrations of PVA in monomeric unit and of CR, respectively. The PVA concentration was fixed to be C_{PVA} = 455 mM. This concentration is close to the sol−gel transition border as shown in Figure 2.

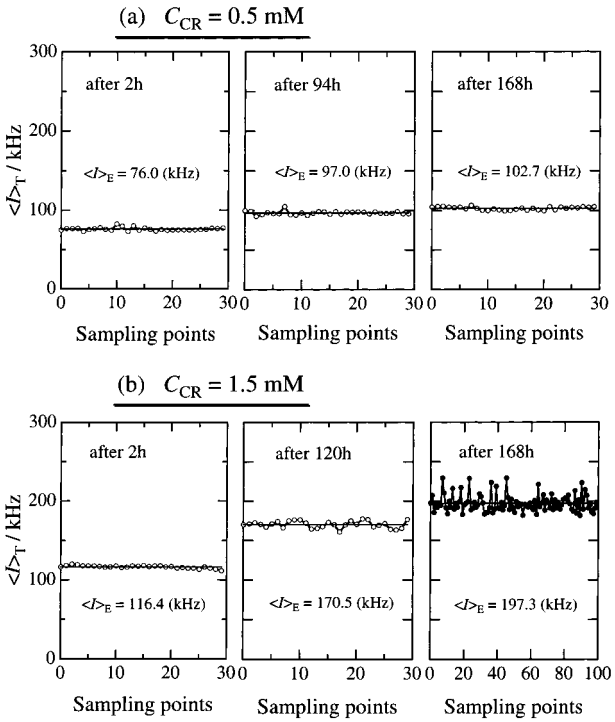

Figure 4. Time evolution of scattered intensity, $\langle I \rangle_T$, variations for PVA/CR systems with (a) C_{CR} = 0.5 and (b) 1.5 mM after quenching from 80 to 20 °C.

SLS/DLS. Dynamic light scattering (DLS) experiments were carried out on a DLS/SLS-5000 (ALV, Co Ltd., Langen, Germany) with a 22 mW He−Ne laser (wavelength, λ = 6328 Å). The sample in a 10 mm test tube was placed in a toluene bath thermostated within an error of ±0.1 °C. The time-averaged scattered intensity, $\langle I \rangle_T$, and its time correlation, i.e., the time-averaged intensity correlation $\langle I(t)I(t+\tau) \rangle_T$, were taken at the scattering angle of 90°. The measurements were repeated at 100 different sampling points per sample at 20 °C in order to obtain ensemble average for each sample having different C_{PVA}'s.

Results and Discussion

1. Gelation Kinetics. In the following two figures, we compare the kinetics of two PVA/CR aqueous solutions with different CR concentrations, i.e., C_{CR} = 0.5 and 1.5 mM. The former remains in sol state, and the latter becomes a gel by aging. Figure 4 shows the time evolution of the scattered intensity variation with sample position, $\langle I \rangle_T$, obtained from PVA/CR aqueous systems with (a) C_{CR} = 0.5 and (b) 1.5 mM, where $\langle I \rangle_T$ is the time average scattered intensity observed at scattering angle of 90°. The solid line indicates the ensemble average scattered intensity, $\langle I \rangle_E$, obtained by

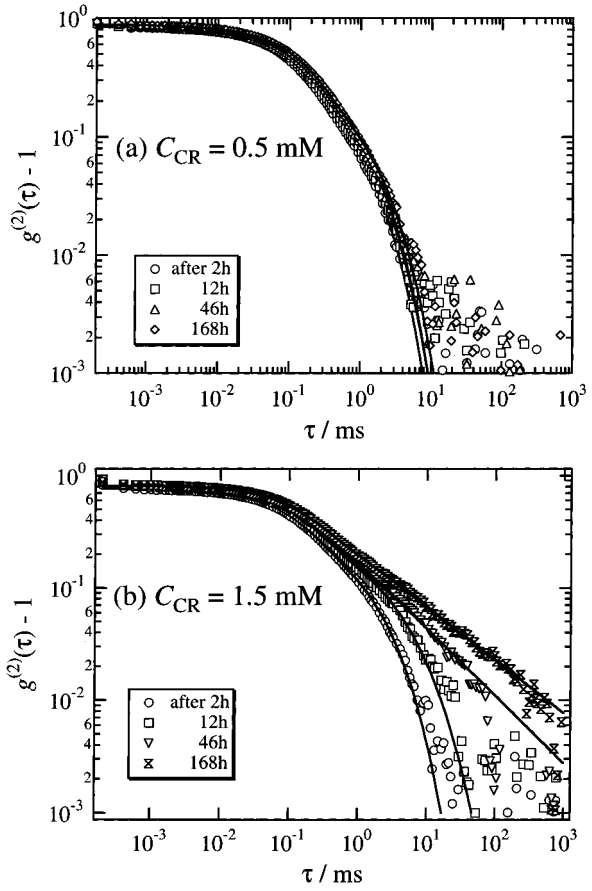

Figure 5. Aging time dependence of time−intensity correlation functions (ICFs) for PVA/CR. (a) C_{CR} = 0.5 and (b) 1.5 mM.

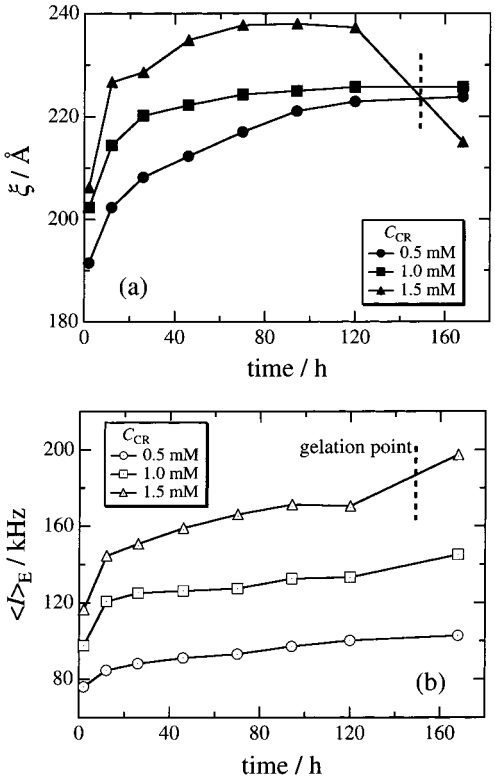

Figure 6. Time evolution of (a) correlation length, ξ, and (b) ensemble average scattered intensity, $\langle I \rangle_E$. The dashed lines indicate where the sol−gel transition occurred for the case of C_{CR} = 1.5 mM.

averaging $\langle I \rangle_T$ with respect to sample positions. It is known that $\langle I \rangle_T$ for sol does not depend on sample position but begins to fluctuate strongly with sample position after gelation.[19−21] Such intensity fluctuations are called speckles. For the case of (a), the system remained in the sol state, and no speckle pattern appeared although $\langle I \rangle_E$ slightly increased with time, t. On the other hand, for the case of (b), $\langle I \rangle_T$ increased with t and started to fluctuate with sample position after t = 168 h. Hence, it was deduced that gelation took place at $t \approx$ 168 h.

In Figure 5 is shown time evolution of the time−intensity correlation function, ICF, for PVA/CR with (a) C_{CR} = 0.5 and (b) 1.5 mM after quenching the sample from 80 °C (sol state) to 20 °C. For the case of C_{CR} = 0.5 mM, ICF did not change with t and could be fitted with a combination of single-exponential and stretched-exponential functions given by[22]

$$g_T^{(2)}(\tau) - 1 \approx \{A \exp(-Dq^2\tau) + (1 - A) \times \exp[-(\tau/\tau_{slow})^{\beta}]\}^2 \quad \text{(for sols)} \quad (1)$$

where D, q, and τ denote the diffusion coefficient of the fast mode, the scattering vector, and the relaxation time, respectively. A is the fraction of the fast mode. τ_{slow} is the characteristic decay time for the slow mode, and β is the stretched exponent.

On the other hand, ICFs for the PVA/CR with C_{CR} = 1.5 mM changed with time as shown in Figure 5b. At t = 46 and 168 h, the ICFs are well described by a combination of a single-exponential and a power-law function,[23]

$$g_T^{(2)}(\tau) - 1 \approx \sigma_I^2\{A \exp(-D_A q^2\tau) + (1 - A)[1 + (\tau/\tau^*)]^{(n-1)/2}\}^2 \quad \text{(for gels)} \quad (2)$$

where σ_I^2 and τ^* are the initial amplitude of ICF and the characteristic time where the power law behavior appears, respectively, and n ($0 < n < 1$) is the fractal dimension of scattered photons.[24] By careful examination of the fit, it is clear that the data points at t = 46 h deviate from the fit around $\tau = 10^2$ ms, while that at t = 168 h is well reproduced by eq 2 in the entire range of τ. Since a power-law behavior is one of the characteristic features of gelation,[25] it was concluded that a gelation took place around t = 168 h. This time is in accordance with that evaluated by the appearance of speckles (Figure 4).

The correlation length, ξ, which is a measure of the spatial correlation can be evaluated from the diffusion coefficient, D,[26]

$$\xi = \frac{kT}{6\pi\eta D} \quad (3)$$

where kT is the Boltzmann energy, η is the solvent viscosity (=0.8945 mPa for water at 20 °C), and D is the collective diffusion coefficient. In a sol state, the diffusion coefficient D in eq 1 can be also evaluated by the initial slope of ICF, i.e.,

$$D = -\frac{1}{2q^2}\frac{\partial}{\partial\tau}\ln[g_T^{(2)}(\tau) - 1]|_{\tau=0} \quad (4)$$

Figure 6a shows time evolution of ξ. The variation of

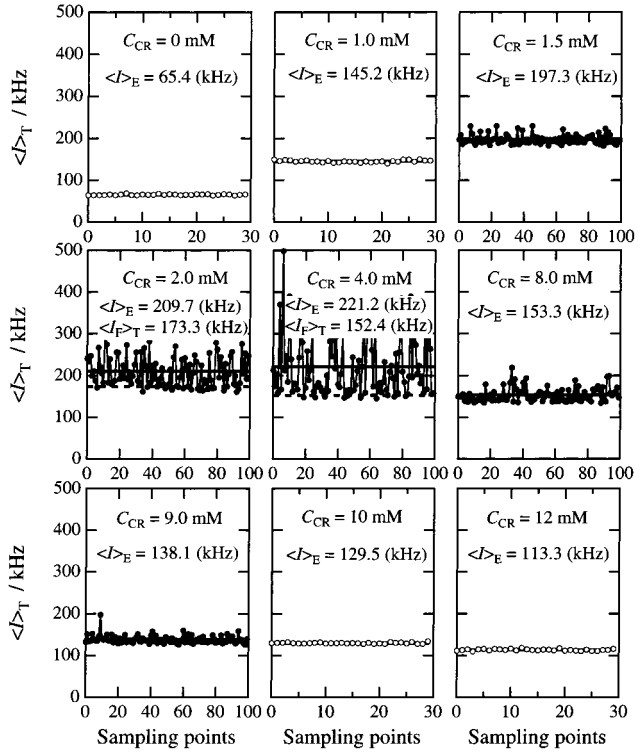

Figure 7. C_{CR} dependence of speckle patters of PVA/CR.

ensemble average scattered intensity, $\langle I\rangle_E$, is also plotted as a function of aging time, t (Figure 6b). Both ξ and $\langle I\rangle_E$ are increasing functions of aging time and indicate that it took roughly 160 h for structural equlibration. The discrete changes of ξ and $\langle I\rangle_E$ across the dashed lines for the case of $C_{CR} = 1.5$ mM are due to sol-to-gel transition and does not mean that the system is not in equilibrium. Hence, we regard that PVA/CR systems aged for more than 160 h are in equilibrium and discuss the mechanism and dynamics of the reentrant sol−gel transition in more detail.

2. C_{CR} Dependence. Figure 7 shows the scattered intensity variation with sample position obtained from aged PVA/CR aqueous systems with $C_{PVA} = 455$ mM and $C_{CR} = 0$, 1.0, 1.5, 2.0, 4.0, 8.0, 9.0, 10.0, and 12 mM. As shown in the figure, speckle patterns appear exclusively in the region $1.5 \le C_{CR} \le 9.0$ mM. This indicates that the system is in a sol state for $C_{CR} \le 1.0$ mM and $C_{CR} > 9$ mM and in a gel state for $1.5 \le C_{CR} \le 9.0$ mM. The change in the scattered intensity variation with C_{CR} is consistent with the macroscopic sol−gel transition determined by tilting-a-tube method (i.e., a flow measurement).

Figure 8 shows a series of intensity−correlation functions (ICF) of PVA/CRs. The shape of ICF changes drastically in the regions $1.0 \le C_{CR} \le 1.5$ mM and $9.0 \le C_{CR} \le 12$ mM and can be classified into three regions, I to III. In regions I ($0 \le C_{CR} \le 1.0$ mM) and III (10 mM $\le C_{CR}$), the ICFs can be fitted with eq 1. On the other hand, in region II ($1.5 \le C_{CR} \le 9.0$ mM), the ICFs are well described with eq 2. According to the previous papers,[15,27] it is clear that ICFs of sols and gels are well described by these two types of functions, i.e., eqs 1 and 2, respectively. Hence, it can be concluded that ICF is another tool to determine the sol−gel transition, and the reentrant sol−gel transition border of PVA/CR is successfully detected.

3. Fast Mode Analysis and Implementation of the Two Transitions. Now, we focus on the fast mode

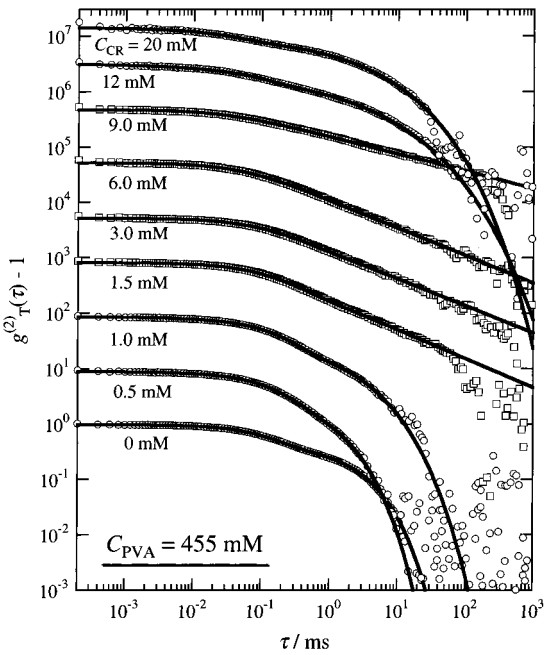

Figure 8. ICFs for PVA/CR ($C_{PVA} = 455$ mM) at various C_{CR}. The shape of ICF differs depending on the sol or gel state.

(the collective diffusion mode). This provides information on the dynamics of entangled and/or cross-linked polymer chains in a blob where spatial correlation reaches. In the case of gels, the ICF for $\tau \ll \tau^*$ consists of homodyne and heterodyne scattering components and is given by a sum of two single-exponential functions as

$$g^{(2)}_T(\tau) - 1 = X^2 \exp(-2Dq^2\tau) + 2X(1 - X) \times \exp(-Dq^2\tau) \quad (\text{for } \tau \ll \tau^*) \quad (5)$$

where X ($\equiv\langle I_F\rangle_T/\langle I\rangle_T$) is the ratio of the intensity from the time-fluctuating component, $\langle I_F\rangle_T$, to the total intensity, $\langle I\rangle_T$, at a given sampling point. The apparent diffusion coefficient, D_A, is simply evaluated by replacing D by D_A in eq 4, but it is now sampling-point-dependent in a gel state. As demonstrated in the previous paper, one can evaluate D and $\langle I_F\rangle_T$ by fitting observed ICFs with eq 5 or by plotting $\langle I\rangle_T/D_A$ vs $\langle I\rangle_T$:[21]

$$\frac{\langle I\rangle_T}{D_A} = \frac{2}{D}\langle I\rangle_T - \frac{\langle I_F\rangle_T}{D} \quad (6)$$

Figure 9 shows the plots for PVA/CR systems with $C_{CR} = 1.0$, 1.5, 3.0, 6.0, 9.0, and 12 mM. The following facts should be noted. The plots are collapsed to a single point for sols ($C_{CR} = 1.0$ and 12 mM), while the data points fall on a straight line given by eq 6, from which D and $\langle I_F\rangle_T$ are quantitatively evaluated.

Figure 10a shows the variation of ξ as a function of C_{CR}. The value of ξ was evaluated from D in terms of eq 3. The vertical dotted lines indicate the sol−gel transition border obtained by the tilting-a-test tube method. Interestingly, ξ changes continuously at the first transition threshold but diverges at the second transition threshold. Therefore, it is deduced that the two transitions seem to have different physical origins. Figure 10b shows the variations of scattered intensities, $\langle I\rangle_E$ and $\langle I_F\rangle_T$. In the gel region, the scattered intensity can be decomposed to the thermal component, $\langle I_F\rangle_T$, and the inhomogeneity component, $\langle I\rangle_E - \langle I_F\rangle_T$. The decrease

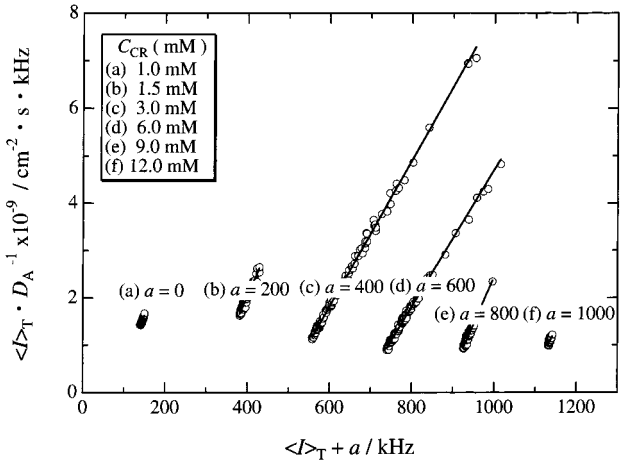

Figure 9. $\langle I \rangle_T / D_A$ vs $\langle I \rangle_T$ plots for PVA/CR with various C_{CR}'s.

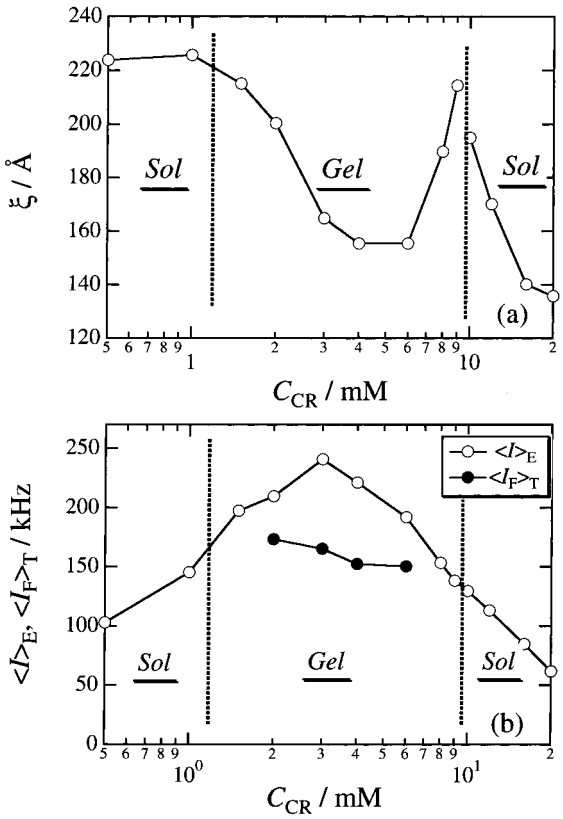

Figure 10. C_{CR} dependence of (a) ξ and (b) $\langle I \rangle_E$ and $\langle I_F \rangle_T$.

in $\langle I_F \rangle_T$ with increasing C_{CR} indicates suppression of thermal concentration fluctuations by increasing cross-linking density.

Figure 11 shows the variations of the averages of the power-law exponent n and the stretched exponent, β. The values of β and n are evaluated exclusively in a sol and gel states, respectively. The decrease in β by approaching the first sol−gel transition indicates that the system becomes more inhomogeneous. By passing the second transition, i.e., the gel-to-sol transition at $C_{CR} \approx 9$ mM, β increases, and the system recovers a more homogeneous structure. On the other hand, the value of n is rather invariant. These behaviors are very different from the case of the concentration-induced sol−gel transition where the value of n changed from 0.3 to 0.6 by approaching the sol−gel transition threshold.[15] This suggests that n is more sensitive to the variation of C_{PVA} rather than that of C_{CR}. This may also indicate

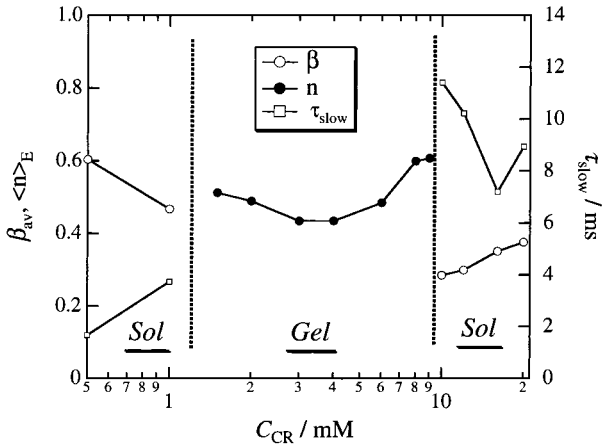

Figure 11. C_{CR} dependence of β_{av}, $\langle n \rangle_E$, and τ_{slow}.

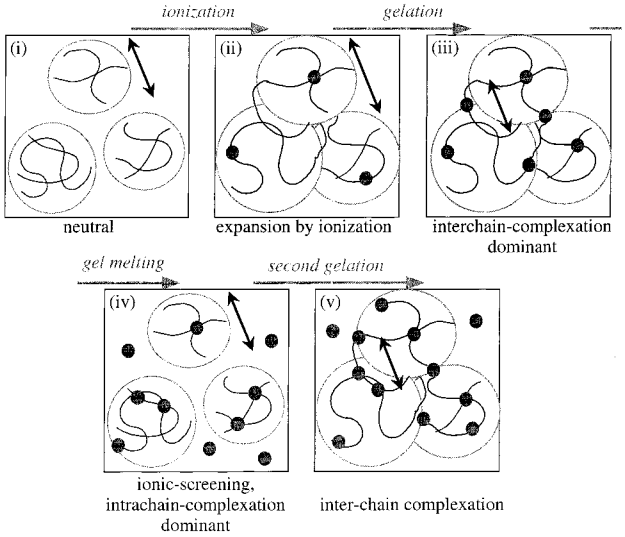

Figure 12. Schematic model explaining the reentrant sol−gel transition.

that n depends on the degree of excluded-volume interaction rather than the degree of ionic shielding.

On the basis of the above results, we conjecture the physical origin of the reentrant sol−gel transition with Figure 12, where solid lines and circles denote PVA chains and CR molecules, respectively. The polymer concentration employed in this work ($C_{PVA} = 455$ mM) is close to the so-called chain overlap concentration $C^* \approx 440$ mM for neutral PVA solutions. Hence, each chain is slightly attached to each other as shown in (i). Complexation with CR leads to ionization of PVA chains, resulting in a shift of C^* to a lower concentration side. As a result, interchain coss-links are formed and gelation takes place (ii). This is the first sol−gel transition. Since the expansion of PVA chains has already occurred by an addition of a slight amount of CR molecules, a further increase in C_{CR} around the first sol−gel transition simply results in a gradual lowering in ξ by cross-linking (iii). Upon further addition of CR, however, ionized CR molecules strongly shield the electrostatic interaction. This results in contraction of individual PVA chains, and intrachain cross-linking becomes dominant. This conjecture is supported by the experimental result on rheological measurements of PVA−CR aqueous complexes.[14] As a result, gel melting takes place (iv). When a larger amount of CR is added to the system, the number of CR ions becomes large enough for gelation. In addition, dominancy of intra-

chain cross-linking is suppressed, which leads to an expansion of PVA chains. Note that the sol−gel transition border is a function of both monomer and cross-linker concentration according to site-bond percolation theory[28] and its experimental verification.[17] Therefore, ξ increases by further increase in C_{CR} and decreases by passing the gelation threshold.

In the previous paper, we discussed the difference in temperature-induced and concentration-induced sol−gel transitions.[15] In the case of the former, the variation of ξ is continuous across the sol−gel transition border, while that for the latter exhibited a cusplike transition. In this study, C_{CR} was varied by keeping C_{PVA} to be close to the so-called overlap concentration. In this case, it is expected that a small variation of C_{CR} drastically affects the sol−gel transition behavior as is found in the case of the concentration-induced sol−gel transition. Furthermore, it should be noted that the degree of ionization of PVA−CR complexes changes significantly by C_{CR}, which results in a shift of the overlap concentration. Therefore, it is easy to expect that a sol−gel transition similar to the concentration-induced sol−gel transition may take place when C_{CR} is scanned, i.e., a cusplike transition.

Conclusion

The microscopic aspects of a reentrant sol−gel transition was investigated for poly(vinyl alcohol)−Congo Red aqueous solutions by dynamic light scattering. Two types of experiments, i.e., the aging experiment and the Congo Red concentration dependence experiment, were carried out. It took roughly 160 h to form a stable gel at 20 °C. The sol−gel transition was detected by the appearance of speckle patterns, i.e., random fluctuations in the scattered intensity with sample position, which is consistent with the sol−gel transition determined macroscopically. The time−intensity correlation function also exhibits a characteristic feature of gelation, i.e., a drastic change from a stretched exponential to a power-law function. In the gel region, the scattered intensity was successfully decomposed to those from thermal fluctuations and from static inhomogeneities. The lowering of the stretched exponent, β, indicates that the system becomes inhomogeneous by approaching the gelation transition. The invariance of the power-law exponent, n, in the gel region indicates that the n is insensitive to C_{CR}. It was found that this result is in contrast with the result of the C_{PVA} induced sol−gel transition. The first sol-to-gel transition is due to an increase of he number of cross-linkers to cross the sol−gel transition border. However, the successive gel-to-sol transition is ascribed to a chain contraction by domination of intrachain cross-linking. The second sol-to-gel transition is due to further increase in cross-linkers to percolate the system. The analysis of the fast-mode of intensity−time correlation function indicates that these sol-to-gel and gel-to-sol transitions are analogous to the temperature-induced and concentration-induced sol−gel transitions, respectively.

Acknowledgment. This work is partially supported by the Ministry of Education, Science, Sports, and Culture, Japan (Grant-in-Aid, 12450388 and 13031019 to M.S.).

References and Notes

(1) Deuel, H.; Neukom, A. *Makromol. Chem.* **1949**, *3*, 113.
(2) Saito, S.; Okuyama, H. *Kolloid Z.* **1954**, *139*, 150.
(3) Crisp, J. D. US Patent 258193, 1946.
(4) Ahad, E. *J. Appl. Polym. Sci.* **1974**, *18*, 1587.
(5) Kawakami, H.; Fujiwara, H.; Kinoshita, Y. Jpn Patent S47-40894, 1972.
(6) Sakurada, I. *Polyvinyl Alcohol Fibers*; Marcel Dekker: New York, 1985.
(7) Shibayama, M.; Adachi, M.; Ikkai, F.; Kurokawa, H.; Sakurai, S.; Nomura, S. *Macromolecules* **1993**, *26*, 623.
(8) Shibayama, M. In *The Polymeric Materials Encyclopedia: Synthesis, Properties, and Applications*; CRC Press: Boca Raton, FL, 1996; Vol. 9, pp 7020−7026.
(9) Leibler, L.; Pezron, E.; Pincus, P. A. *Polymer* **1988**, *29*, 1105.
(10) Pezron, E.; Leibler, L.; Ricard, A.; Lafuma, F.; Audebert, R. *Macromolecules* **1989**, *22*, 1169.
(11) Beltman, H.; Lyklema, J. *Faraday Discuss. Chem. Soc.* **1974**, *57*, 92.
(12) Shibayama, M.; Ikkai, F.; Moriwaki, R.; Nomura, S. *Macromolecules* **1994**, *27*, 1738.
(13) Shibayama, M.; Ikkai, F.; Nomura, S. *Macromol. Symp.* **1994**, *93*, 277.
(14) Shibayama, M.; Moriwaki, R.; Ikkai, F.; Nomura, S. *Polymer* **1994**, *26*, 5716.
(15) Shibayama, M.; Tsujimoto, M.; Ikkai, F. *Macromolecules* **2000**, *33*, 7868.
(16) Norisuye, T.; Takeda, M.; Shibayama, M. *Macromolecules* **1998**, *31*, 5316.
(17) Takeda, M.; Norisuye, T.; Shibayama, M. *Macromolecules* **2000**, *33*, 2909.
(18) Norisuye, T.; Shibayama, M.; Tamaki, R.; Chujo, Y. *Macromolecules* **1999**, *32*, 1528.
(19) Pusey, P. N.; van Megen, W. *Physica A* **1989**, *157*, 705.
(20) Joosten, J. G. H.; McCarthy, J. L.; Pusey, P. N. *Macromolecules* **1991**, *24*, 6690.
(21) Shibayama, M.; Fujikawa, Y.; Nomura, S. *Macromolecules* **1996**, *29*, 6535.
(22) Ren, S. Z.; Shi, W. F.; Zhang, W. B.; Sorensen, C. M. *Phys. Rev. A* **1992**, *45*, 2416.
(23) Martin, J. E.; Wilcoxon, J. *Phys. Rev. Lett.* **1988**, *61*, 373.
(24) Martin, J. E.; Wilcoxon, J.; Odinek, J. *Phys. Rev. A* **1991**, *43*, 858.
(25) Norisuye, T.; Inoue, M.; Shibayama, M.; Tamaki, R.; Chujo, Y. *Macromolecules* **2000**, *33*, 500.
(26) Tanaka, T. In *Dynamic Light Scattering*; Pecora, R., Ed.; Plenum Publishing: New York, 1985; pp 347−362.
(27) Ikkai, F.; Shibayama, M. *Phys. Rev. Lett.* **1999**, *82*, 4946.
(28) Coniglio, A.; Stanley, H. E. *Phys. Rev. Lett.* **1979**, *42*, 518.

MA011175B